SUPPORTING INFORMATION

Synthesis and Hydrolysis of Gas-Phase Lanthanide and Actinide Oxide Nitrate Complexes: A Correspondence to Trivalent Metal Ion Redox Potentials and Ionization Energies

Ana F. Lucena,[a] Célia Lourenço,[a] Maria C. Michelini,[b,]* Philip X Rutkowski,[c] José M. Carretas,[a] Nicole Zorz,[d] Laurence Berthon,[d] Ana Dias,[e] M. Conceição Oliveira,[e] John K. Gibson,[b] Joaquim Marçalo[a,]*

[a] *Centro de Ciências e Tecnologias Nucleares, Instituto Superior Técnico, Universidade de Lisboa, 2695-066 Bobadela LRS, Portugal*

[b] *Dipartimento di Chimica, Università della Calabria, 87030 Arcavacata di Rende, Italy*

[c] *Chemical Sciences Division, Lawrence Berkeley National Laboratory, Berkeley, CA 94720, USA*

[d] *CEA, Nuclear Energy Division, Radiochemistry and Processes Department, Laboratory of Ligands-Actinides Interactions, 30207 Bagnols-sur-Cèze, France*

[e] *Centro de Química Estrutural, Instituto Superior Técnico, Universidade de Lisboa, 1049-001 Lisboa, Portugal*

* Corresponding authors: mc.michelini@unical.it; jmarcalo@ctn.ist.utl.pt

Complete Reference 38:

Gaussian 09, Revision B.01, Frisch, M. J.; Trucks, G. W.; Schlegel, H. B.; Scuseria, G. E.; Robb, M. A.; Cheeseman, J. R.; Scalmani, G.; Barone, V.; Mennucci, B.; Petersson, G. A.; Nakatsuji, H.; Caricato, M.; Li, X.; Hratchian, H. P.; Izmaylov, A. F.; Bloino, J.; Zheng, G.; Sonnenberg, J. L.; Hada, M.; Ehara, M.; Toyota, K.; Fukuda, R.; Hasegawa, J.; Ishida, M.; Nakajima, T.; Honda, Y.; Kitao, O.; Nakai, H.; Vreven, T.; Montgomery, J. A., Jr.; Peralta, J. E.; Ogliaro, F.; Bearpark, M.; Heyd, J. J.; Brothers, E.; Kudin, K. N.; Staroverov, V. N.; Kobayashi, R.; Normand, J.; Raghavachari, K.; Rendell, A.; Burant, J. C.; Iyengar, S. S.; Tomasi, J.; Cossi, M.; Rega, N.; Millam, M. J.; Klene, M.; Knox, J. E.; Cross, J. B.; Bakken, V.; Adamo, C.; Jaramillo, J.; Gomperts, R.; Stratmann, R. E.; Yazyev, O.; Austin, A. J.; Cammi, R.; Pomelli, C.; Ochterski, J. W.; Martin, R. L.; Morokuma, K.; Zakrzewski, V. G.; Voth, G. A.; Salvador, P.; Dannenberg, J. J.; Dapprich, S.; Daniels, A. D.; Farkas, Ö.; Foresman, J. B.; Ortiz, J. V.; Cioslowski, J.; Fox, D. J. Gaussian, Inc., Wallingford CT, 2009.

Table S1. Electron density (ρ_{BCP}), Laplacian of electron density ($\nabla^2\rho_{BCP}$), and total energy density (H_{BCP}) for the M-OH BCP of $M(OH)(NO_3)_3^-$ and the M-O BCP of $MO(NO_3)_3^-$ complexes; M = La, Ce, Pr, Lu, Al, Sc, and Y.[a, b,c]

$M(OH)(NO_3)_3^-$	La (1)	Ce (2)	Pr (3)	Lu (1)	Al (1)	Sc (1)	Y (1)
ρ_{BCP}	0.0930 [0.0938]	0.0942 [0.0958]	0.0956	0.1065	0.0994 [0.1068]	0.1105	0.0865
$\nabla^2\rho_{BCP}$	0.3712 [0.3770]	0.4005 [0.4041]	0.4169	0.5714	0.8060 [0.7642]	0.6360	0.4777
H_{BCP}	-0.0191 [-0.0193]	-0.0172 [-0.0191]	-0.0176	-0.0237	0.0013 [-0.0014]	-0.0104	-0.0064
DI(M,O)	0.715 [0.709]	0.733 [0.725]	0.736	0.618	0.341 [0.330]	0.680	0.595
$d_{M\text{-}OH}$[d]	2.15	2.13	2.12	2.00	1.72	1.89	2.05
$MO(NO_3)_3^-$	La (2)	Ce (1)	Pr (2)[e]	Lu (2)	Al (2)	Sc (2)	Y (2)
ρ_{BCP}	0.0893 [0.0900]	0.2563 [0.2576]	0.2223	0.1001	0.0926 [0.0993]	0.1059	0.0806
$\nabla^2\rho_{BCP}$	0.2526 [0.2532]	0.2645 [0.2380]	0.3241	0.4089	0.6813 [0.6443]	0.4775	0.3360
H_{BCP}	-0.0199 [-0.0210]	-0.2060 [-0.2126]	-0.1519	-0.0242	-0.0011 [-0.0015]	-0.0127	-0.0073
DI(M,O)	0.693 [0.682]	1.946 [1.920]	1.779	0.598	0.343 [0.329]	0.671	0.585
$d_{M\text{-}O}$[d]	2.26	1.80	1.85	2.09	1.77	1.96	2.16

[a]In atomic units. [b] Spin multiplicity in parentheses. [c]With the aim of analyzing the basis sets effect on AIM properties, single point B3LYP/SDD(Ln):6-311++(2df,2dp) (rest of the atoms) were performed on the B3LYP/SDD(An):6-311++(d,p) optimized geometries, on selected cases. The AIM properties at this level of theory are reported in square brackets. [d]Metal-oxygen bond lengths in angstroms. [e] The antiferromagnetically coupled doublet spin state isomer (19 $kJ.mol^{-1}$ higher in energy, $d_{Pr\text{-}O}$ = 2.19Å) has topological characteristics similar to those of $LaO(NO_3)_3^-$ and $LuO(NO_3)_3^-$ oxides.

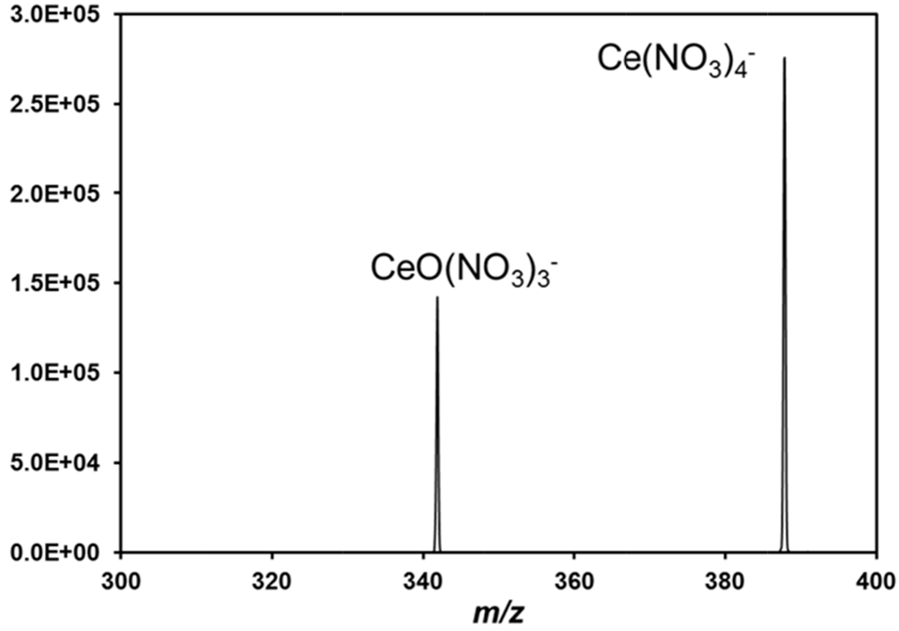

Figure S1. CID mass spectrum of $Ce(NO_3)_4^-$ (C2TN-IST).

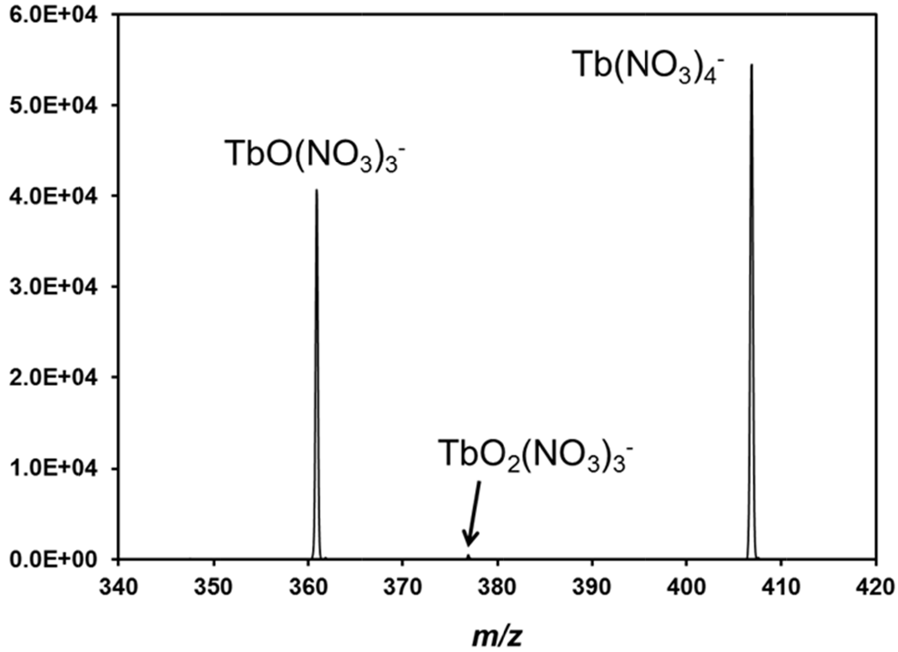

Figure S2. CID mass spectrum of $Tb(NO_3)_4^-$ (C2TN-IST).

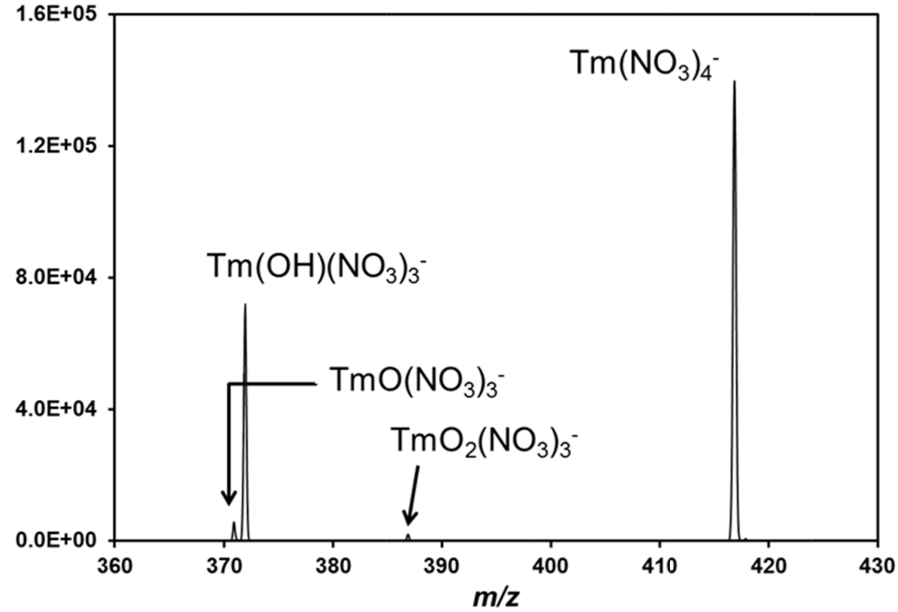

Figure S3. CID mass spectrum of $Tm(NO_3)_4^-$ (C2TN-IST).

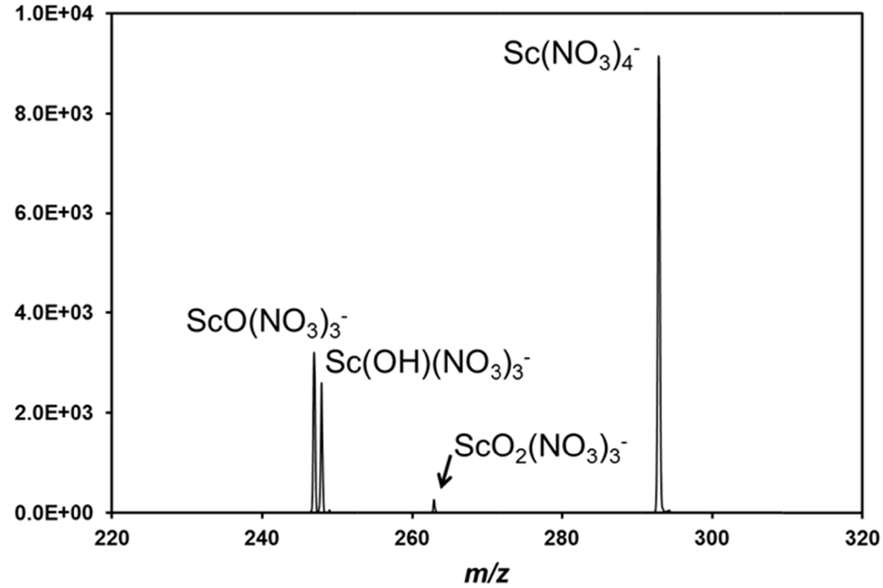

Figure S4. CID mass spectrum of $Sc(NO_3)_4^-$ (C2TN-IST).

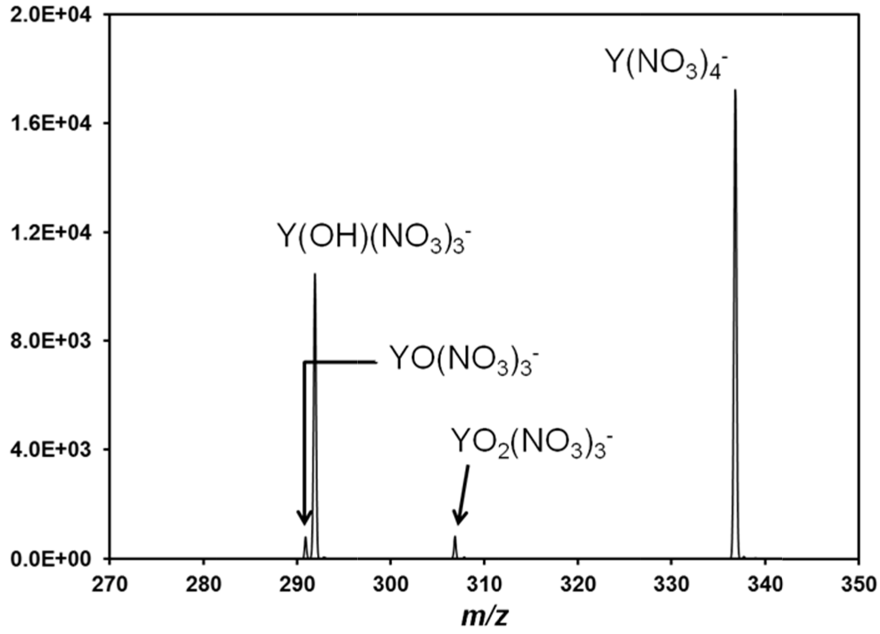

Figure S5. CID mass spectrum of $Y(NO_3)_4^-$ (C2TN-IST).

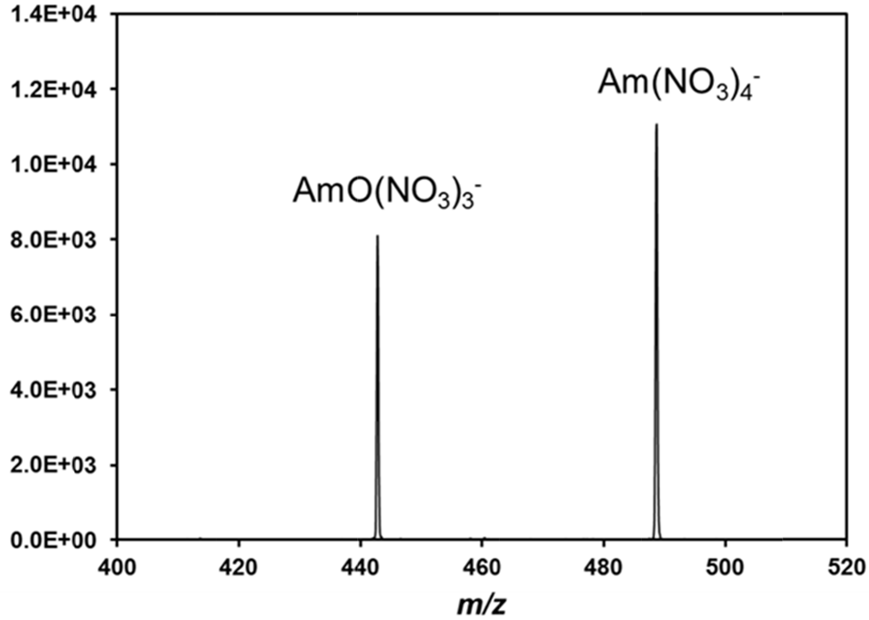

Figure S6. CID mass spectrum of $Am(NO_3)_4^-$ (CEA).

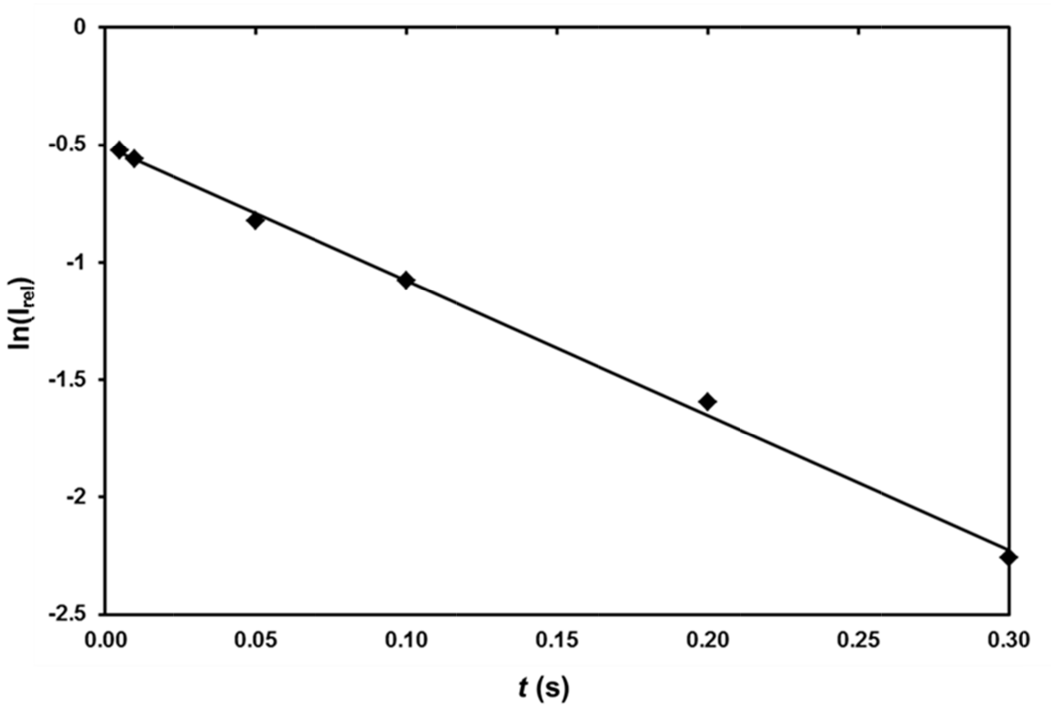

Figure S7. Kinetic plot from the reaction of isolated $HoO(NO_3)_3^-$ with H_2O to form $Ho(OH)(NO_3)_3^-$, obtained at CQE-IST (R^2 = 0.9977).